

# Energy harvesting using an aerodynamic blade element at resonant frequency with air excitation

Fevzi C. Bolat<sup>1</sup> and Selim Sivrioglu<sup>\*2</sup>

<sup>1</sup>Department of Mechanical Engineering, Bolu Abant İzzet Baysal University, Bolu, Turkey

<sup>2</sup>Department of Mechanical Engineering, Gebze Technical University, Gebze, Turkey

(Received January 5, 2019, Revised July 25, 2019, Accepted August 6, 2019)

**Abstract.** In this research, we propose an energy harvesting structure with a flexible blade element vibrating at its first mode to maximize the power output of the piezoelectric material. For this purpose, a piezoelectric patch was attached on the blade element used in a small-scale wind turbine, and air load was applied with a suitable angle of attack in the stall zone. The aerodynamic load created by air excitation vibrates the blade element in its first natural frequency and maximizes the voltage output of the piezoelectric patch. The variation of power outputs with respect to electrical resistance, air speed, and extra mass is experimentally investigated for various cases. An analytical model is constituted using a single-mode blade element with piezoelectric patch dynamics, and the power outputs of the obtained model are compared with experimental results.

**Keywords:** piezo-aeroelastic structure; energy harvesting; flexible structure; aerodynamic excitation

## 1. Introduction

The increasing energy demand in daily life with the extensive number of technological devices has been accelerating renewable energy studies. Not only large amount of energy production any small level of energy production also gains importance. Recently, piezoelectric materials have attracted much attention for energy harvesting systems. Piezoelectric materials produce a voltage when subjected to strain and efficiently transform mechanical energy into electrical energy. If a source of mechanical motion exists, the piezoelectric material bonded to a surface and exposed to this mechanical movement can give a continuous voltage output. Wind sources may be used in piezoelectric material-based energy harvesting systems by creating vibration of structures apart from the conventional rotating motion of wind turbines.

In the literature, earlier studies on energy harvesting from piezoelectric material use generally a non-aerodynamic beam element to attach the piezoelectric patch and a shaker for the source of vibration. Energy harvesting studies (Erturk and Inman 2009, Bryant *et al.* 2011, Casciati *et al.* 2012, Zhao and Yang 2017, Latif *et al.* 2018, Bolat *et al.* 2019) have proposed a piezoelectric material attached beam which was actuated by a shaker at different frequencies to analyze the energy outputs. Sousa *et al.* (2011) performed analytical and experimental studies to obtain piezoaeroelastic energy harvesting linear and nonlinear models.

As a source of vibration, different types of structures were examined generally with air load. Vatansever *et al.* (2011) investigated the energy harvesting efficiency of PZT and PVDF materials using two different experimental methods. The first of these methods was to drop water on the piezoelectric beam, and the other was to place the beam in an air canal and examine its behavior at different speeds. Sirohi and Maradik (2011) examined the energy harvest by applying an air load on a triangular cross-section beam which was attached to two other beams having the piezoelectric patch. They also derived an analytical model for the proposed energy harvesting structure and examined the aerodynamic effects. Abdelkefi *et al.* (2013) fixed a piezoelectric patch on two beams and connected them with another beam that had a triangular cross-section. They applied an air load on the triangular cross-section beam to generate vibrations in the piezoelectric beams and harvest energy.

Several studies used an airfoil to vibrate the piezoelectric patch attached beam with air load. Bryant *et al.* (2011, 2011) studied a PZT patch attached beam having an airfoil mounted at the end of it and realized the energy harvesting operation experimentally by applying wind load. This study also examined the determination of the minimum air speed required for the airfoil vibration movement. In addition, linear and nonlinear mathematical models were obtained for the proposed energy harvesting system, and the models were compared with experimental results. Erturk *et al.* (2010) extracted a mathematical model for an aeroelastic energy harvest system with a piezoelectric patch and conducted experimental validation of the obtained model. Marquri and Erturk (2013) worked on two different types of energy harvesting methods by connecting an airfoil profile on the beam. One of these methods is to generate energy from the piezoelectric patch by vibrating the beam with an air load. The other is placing a magnet on the vibrating

\*Corresponding author, Professor

E-mail: [s.selim@gtu.edu.tr](mailto:s.selim@gtu.edu.tr)

<sup>a</sup> Ph.D.

E-mail: [fevzibolat@bayburt.edu.tr](mailto:fevzibolat@bayburt.edu.tr)

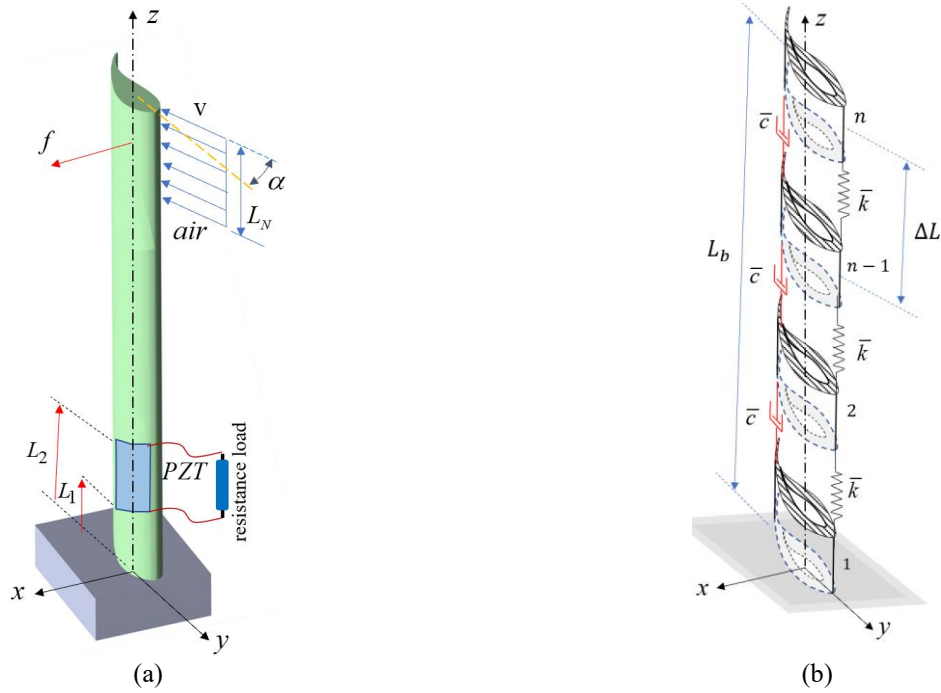


Fig. 1 Aeroelastic blade structure (a) layout of the blade and (b) lump-parameter model

beam and fixing a coil against it and harvesting energy from the coil. Concerning with the airfoil attached studies, Bibo *et al.* (2013, 2013) examined the behavior of air load and base excitation by connecting an airfoil member to the end point of the beam element. They also analyzed the amount of energy obtained from the piezoelectric patch adhered to the beam by giving different air velocities.

In recent studies, to increase the amount of harvested energy, Javed *et al.* (2016) tried to increase mechanical vibration with aeroelastic effect on a multi-piezo beam mechanism. Tsushima and Su (2016) investigated energy harvesting from the transient vibrations of thin wing geometry under aerodynamic effect. In the study, mathematical models were extracted in many respects and the efficiency of the proposed structure was examined considering the nonlinear effects in the simulation environment.

In this study, a new energy harvesting structure is proposed using a highly flexible small-scale blade element oscillating at resonant frequency. It is aimed to maximize the power output of the attached piezoelectric patch by vibrating the blade element with aerodynamic wind loads. A wind turbine blade element with high flexibility has not been studied experimentally for energy harvesting purposes in the literature.

## 2. Blade element mathematical model

A flexible blade element with attached PZT patch illustrated in Fig. 1(a) is used for energy harvesting purposes. The blade element has an aerodynamic form with an airfoil coded SH3055 which was designed for small wind energy turbines. The setup is experimentally excited at

the end with an air nozzle to have oscillation at a certain vibration mode. An equation of motion of the cantilever blade element was derived using the lumped-parameter modeling approach. The blade element has longitudinally a uniform mass distribution and is separated into equal segments of the same length as illustrated in Fig. 1(b). For each element of the blade, a bending stiffness is calculated. The equation of motion is derived as

$$M\ddot{x} + Kx = f \quad (1)$$

where  $M$  is the mass matrix and  $K$  is the stiffness matrix. If a linear damping is considered, the damping matrix can be constructed with a linear combination of the mass and stiffness matrices such as  $C = \chi M + \gamma K$ , and  $\chi, \gamma$  are constants. The extended model is written as

$$M\ddot{x} + C\dot{x} + Kx = f \quad (2)$$

A transformation from the physical coordinate to the modal coordinate is realized as follows

$$\ddot{\eta} + \Lambda\dot{\eta} + \Omega^2\eta = f_0 \quad (3)$$

The modal matrix  $\Phi$  is used to transform the system matrices of  $I = \Phi^T M \Phi$ ,  $\Omega^2 = \Phi^T K \Phi$ ,  $\Lambda = 2\zeta \Omega$  and  $f_0 = \Phi^T f$ .

To maximize the energy output the blade is forced to vibrate at its resonant frequency using an air excitation. To determine the natural frequency of the blade element an analysis was experimentally performed and compared with the obtained mathematical model and Ansys program results. For the numerical analysis of the blade profile, a three-dimensional model of the blade was created by using computer-aided design (CAD) software SolidWorks and transferred to Ansys Workbench finite element software. The blade element is divided into 14958 elements with sweep mesh method. Using

Table 1 Natural frequency of the blade element

Lumped model results [Hz]	ANSYS results [Hz]	Experimental results [Hz]
9.94	10.15	9.50
61.12	63.04	59.75
167.06	178.20	167.00

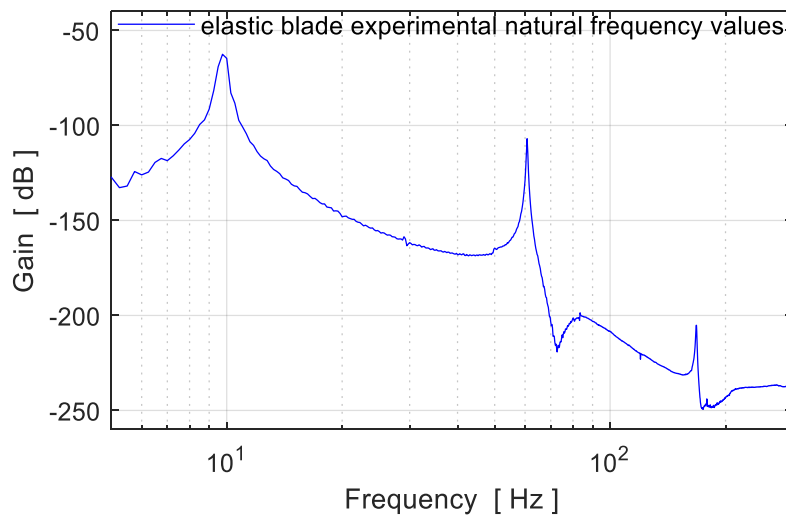


Fig. 2 Experimental frequency response of the blade

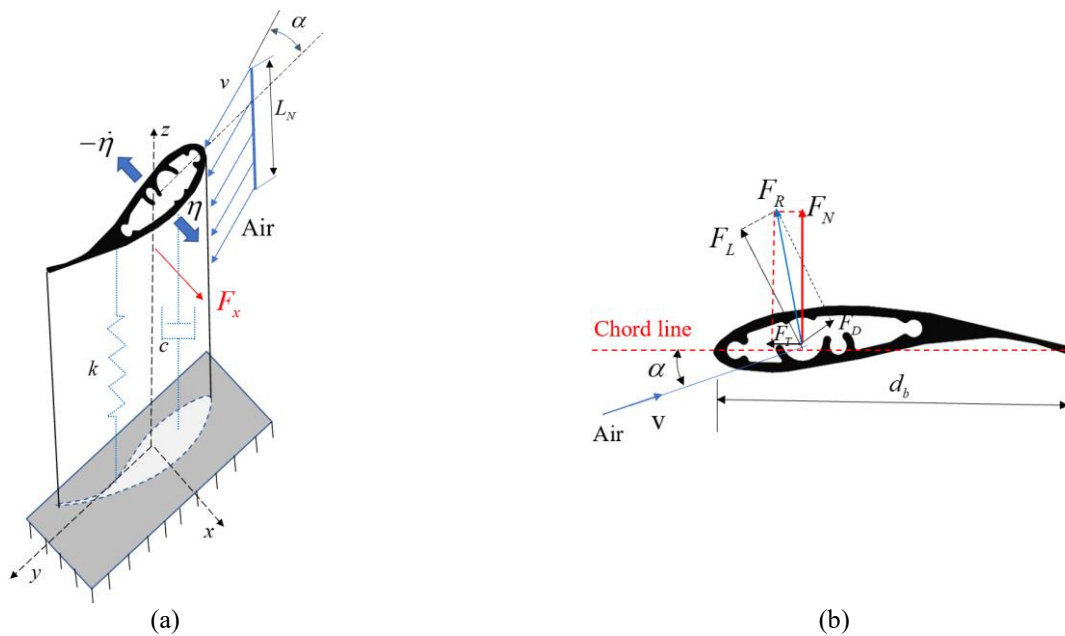


Fig. 3 Schematics of energy harvesting (a) single mode blade model and (b) aerodynamic forces

the modal analysis mode of the Ansys, the natural frequencies of the blade element model were obtained. The natural frequencies are shown in Table 1 for the first three vibration modes. Also, the measured experimental frequency response of the flexible blade is given in Fig. 2.

### 3. Piezoaeroelastic model

The blade element was vibrated at the first natural frequency and the energy harvested. Consider the first vibration mode of the blade model obtained Eqs. (3)

Table 2 Parameters of the cantilever blade and PZT patch

Symbol	Meaning	Value	Unit
$E_b$	Young's modulus of the blade	65	GPa
$d_b$	Chord width of the blade	0.05	M
$L_p$	Length of the PZT patch	0.050	M
$L_b$	Length of the blade	0.8	M
$b_p$	Width of the PZT patch	0.030	M
$h_p$	Thickness of the PZT patch	0.0005	M
$h_b$	Thickness of the blade	0.009	M
$d_{31}$	Piezoelectric charge constant	$-1.8 \times 10^{-10}$	C/N
$\rho_p$	Density of the PZT patch	7800	kg/m <sup>3</sup>
$E_p$	Young's modulus of the PZT patch	6.2	GPa
$L_N$	Aerodynamic force length	0.1	M

according to modal coordinates. The schematic illustration of the single mode energy harvesting model is shown in Fig. 3(a). The equation of motion for the aeroelastic energy harvest structure is written as follows

$$\begin{aligned} \ddot{\eta}_1(t) + 2\xi_1\omega_{n1}\dot{\eta}_1(t) + \omega_{n1}^2\eta_1(t) - \theta_1V(t) &= -F_x(t) \\ C_p\dot{V}(t) + \frac{V(t)}{R} + \theta_1\dot{\eta}_1(t) &= 0 \end{aligned} \quad (4)$$

where  $\eta_1$ ,  $\dot{\eta}_1$ ,  $\ddot{\eta}_1$  are modal displacement, velocity and acceleration of the blade element,  $\theta_1$  is the electromechanical coupling coefficient,  $C_p$  is the capacitance of the piezoelectric layer, and  $F_x$  is the aerodynamic force. Also,  $\omega_{n1}$  is the first mode natural frequency of the blade,  $\xi_1$  is the damping ratio of the first vibration mode.

The energy obtained from the piezoelectric material for open circuit voltage is written as  $v_p = -2d_{31}b_p(h_p + h_b)$ . Here  $h_p$  is the thickness of the piezoelectric layer,  $d_{31}$  is the piezoelectric strain constant. The electromechanical coupling term is given as  $\theta = \psi_n'(L_p)v_p$  where  $\psi_n$  is the mode shape function of the flexible blade element. The energy is obtained from the piezoelectric material under an air input. The electrical capacitance is given by  $C_p = (4\varepsilon^s_{33}b_p(L_p))/h_p$ . Here  $\varepsilon^s_{33}$  is the permittivity constant of the piezoelectric material.

When an air current flows over the aerodynamic blade element with a certain angle of attack  $\alpha$ , a lift force  $F_L$  and a drag force  $F_D$  occur as shown in Fig. 3(b). A resultant force  $F_R$  can be obtained using these forces. The components of the resultant force are the normal  $F_N$  and tangential force  $F_T$ . The normal force is also called the axial force and can be defined as

$$F_N = F_L \cos(\alpha) + F_D \sin(\alpha) \quad (5)$$

where the lift and drag forces are  $F_L = \frac{1}{2}C_L\rho L_N d_b v^2$ ,  $F_D = \frac{1}{2}C_D\rho L_N d_b v^2$ . Finally, the effective aerodynamic force  $F_x$  is written as

$$F_x = -\frac{1}{2}\rho v^2 d_b L_N [C_L \cos(\alpha) + C_D \sin(\alpha)] \quad (6)$$

where  $C_L$  is the lift coefficient,  $C_D$  is the drag coefficient,  $L_N$  is the aerodynamic excitation dimension of the blade normal to the incoming flow and  $\rho$  is the fluid density. Also,  $d_b$  is the width of the blade and  $v$  is the relative wind speed. The parameter values of the blade and PZT patch are given in Table 2.

#### 4. Experimental study

The experimental system is established as shown in Fig. 4. In the experimental setup, a PI 876 A.12 DURACT piezoelectric material is used for energy harvesting. The PZT patch is attached on the flexible blade element at near to the clamp side. The natural frequency of the blade is measured with a 12-channel Bruel & Kjaer vibration analyzer device. The instantaneous displacement information of the blade by the effect of the air load is measured by an optical sensor and processed on the dSPACE 1104 control card. Power supplies, an air valve and an oscilloscope are other peripheral equipment used in the experimental system.

##### 4.1 Aerodynamic excitation

To harvest and maximize energy from the PZT patch, the flexible blade element must vibrate at its first natural frequency with an air excitation. The air excitation generates a steady state vibration on the blade element. The detailed view of the air nozzle and the blade structure is shown in Fig. 5. The air nozzle set to blow the air with a prescribed speed towards the end of the blade as illustrated in Fig. 5. The lift and drag coefficients of the SH3055 airfoil reported in reference (Somers and Maughmer 2003) vary with the angle of attack. Using the SH3055 airfoil data the flow over the airfoil stalls around at an angle of attack of 14 degrees. In the experimental system, the angle of attack of the air nozzle is set to 17.2 degrees (Bolat and

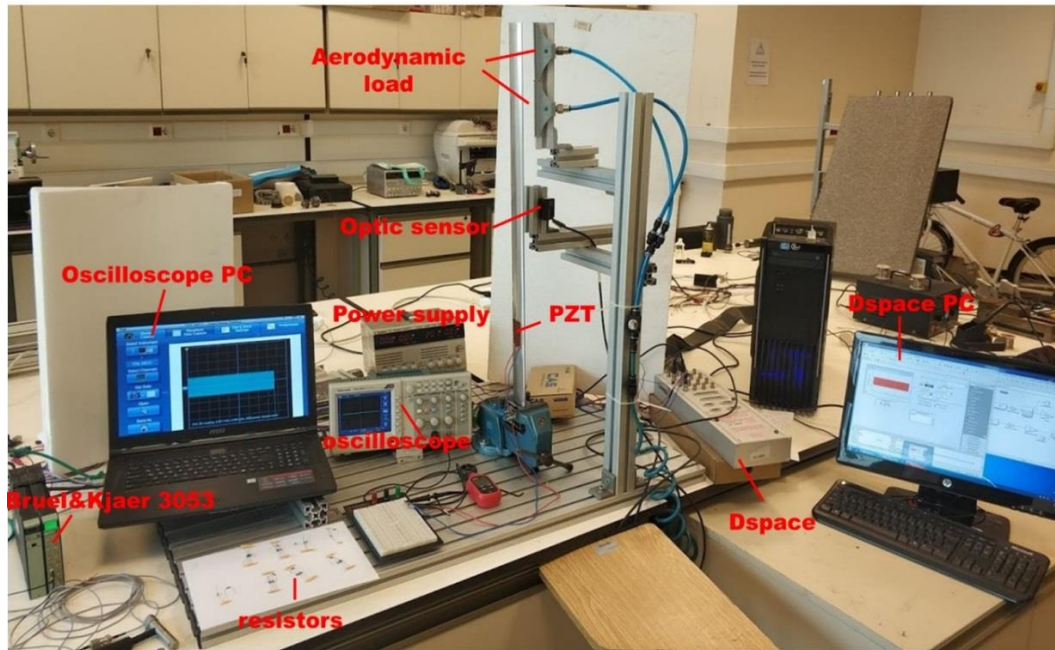


Fig. 4 A view of of the experimental system

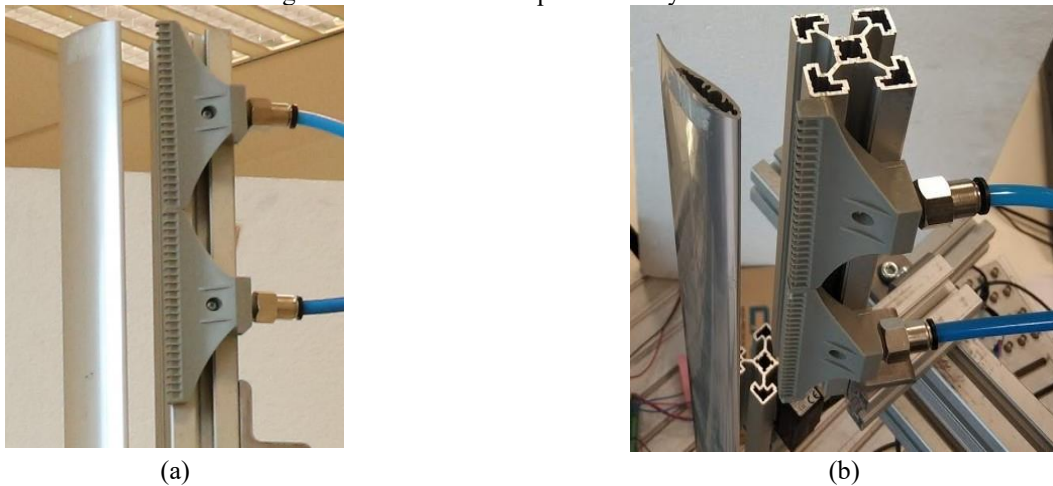


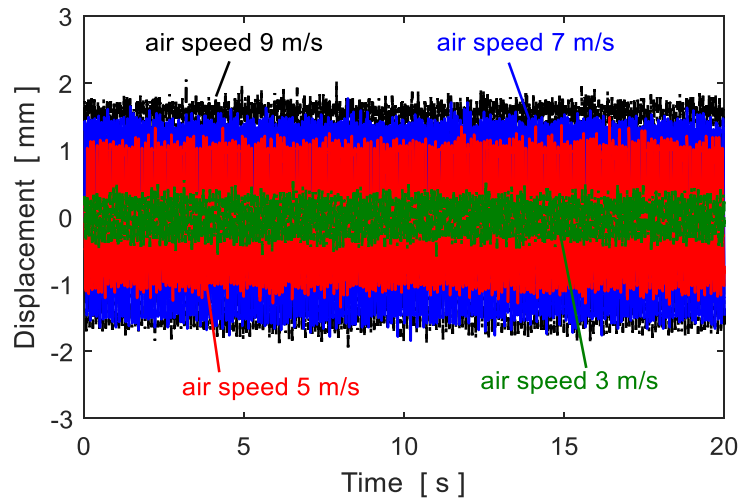
Fig. 5 View of the air nozzle and the blade structure (a) side view and (b) top view

Sivrioglu 2018). It is important to create a steady state vibration for the blade element so that the PZT patch give a continuous output. In our repeated experimental tests, the stall occurred at the set angle of attack for different air speeds. When the air flow over an airfoil stalls, it separates from the surface of the airfoil and the vortex shedding creates fluctuations in the lift causing vibrations on the blade structure. Usman *et al.* (2018) examined the relationship between aerodynamic effect and energy harvest. They studied a novel piezoelectric energy harvesting system using the wake galloping phenomenon for the broad wind spectrum.

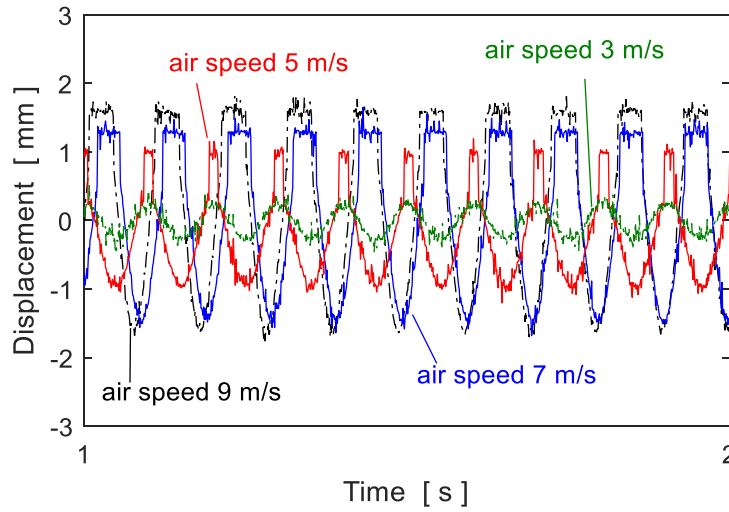
#### 4.2 Air velocity effect

The excitation frequency of the air load is almost equal

to the first natural frequency of the blade obtained by experimentally. Therefore, energy harvesting in the resonance region is maximized due to a steady state vibration of the flexible blade given in Fig. 6(a). Experimental results given in Fig. 6(b) showed that the increase in air velocity did not affect the total number of cycles per second, but it affects the amplitude value. Fig. 7 shows the voltage change at four different air velocities. Depending on the increase in air velocity, voltage outputs increase at the same time as seen in Fig. 7. It is observed in Fig. 8 that the current outputs increase at the same time due to the increase of air speed. Fig. 9(a) and 9(b) shows the current and voltage variations under different speeds of air flow.



(a)



(b)

Fig. 6 Effect of different air velocities on the blade displacement (a) long range and short range

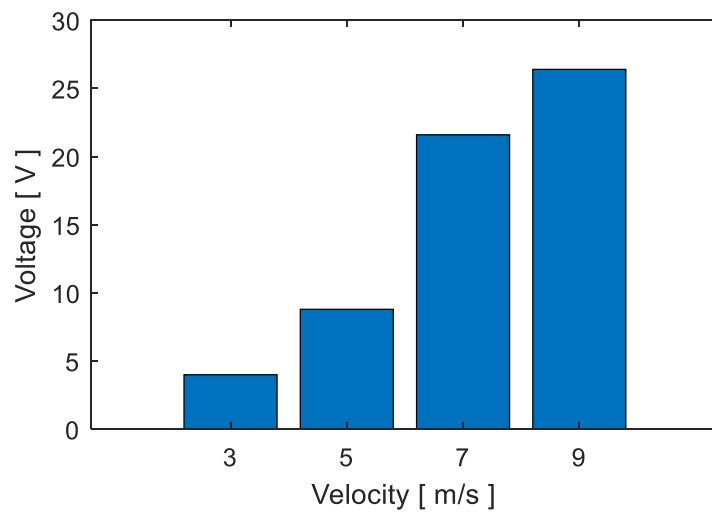


Fig. 7 Effect of different air velocities on the voltage output

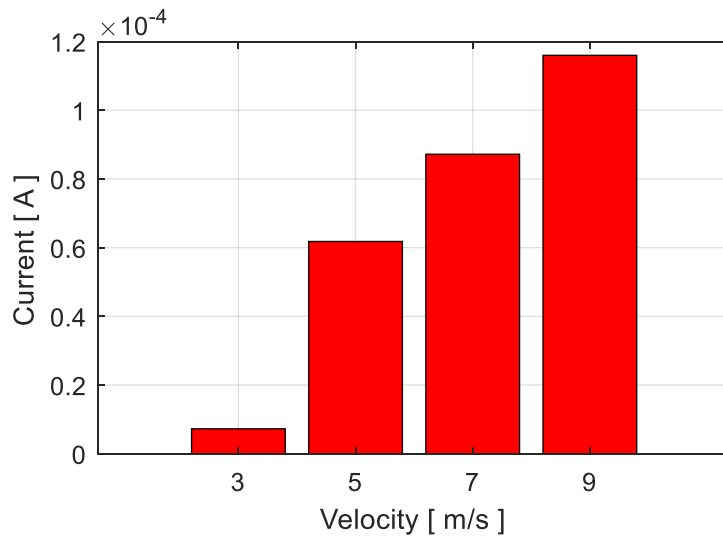


Fig. 8 Effect of different air velocities on the current output

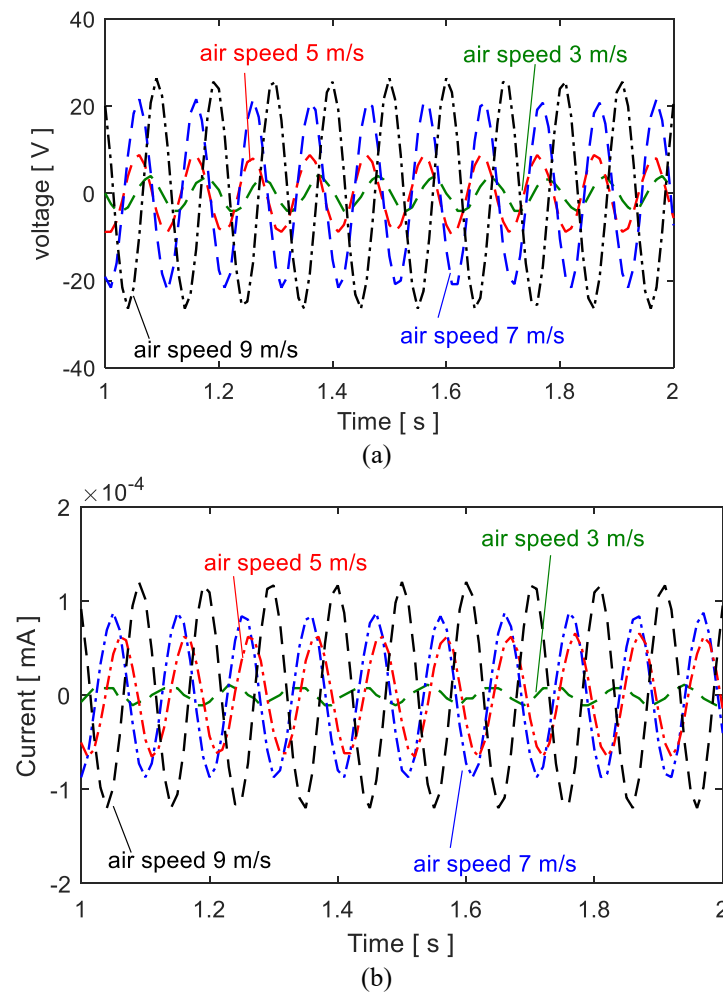


Fig. 9 Effect of different air velocities on (a) voltage responses and (b) current responses

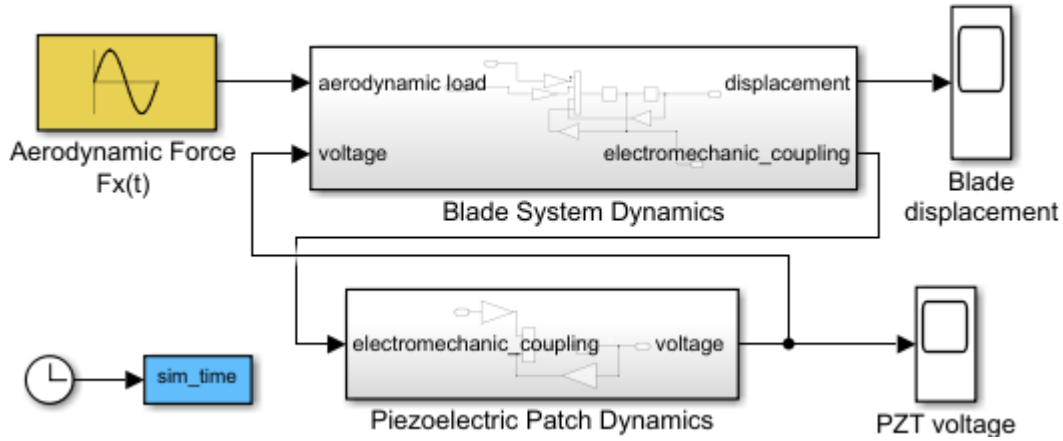


Fig. 10 The Matlab/Simulink model used in the study

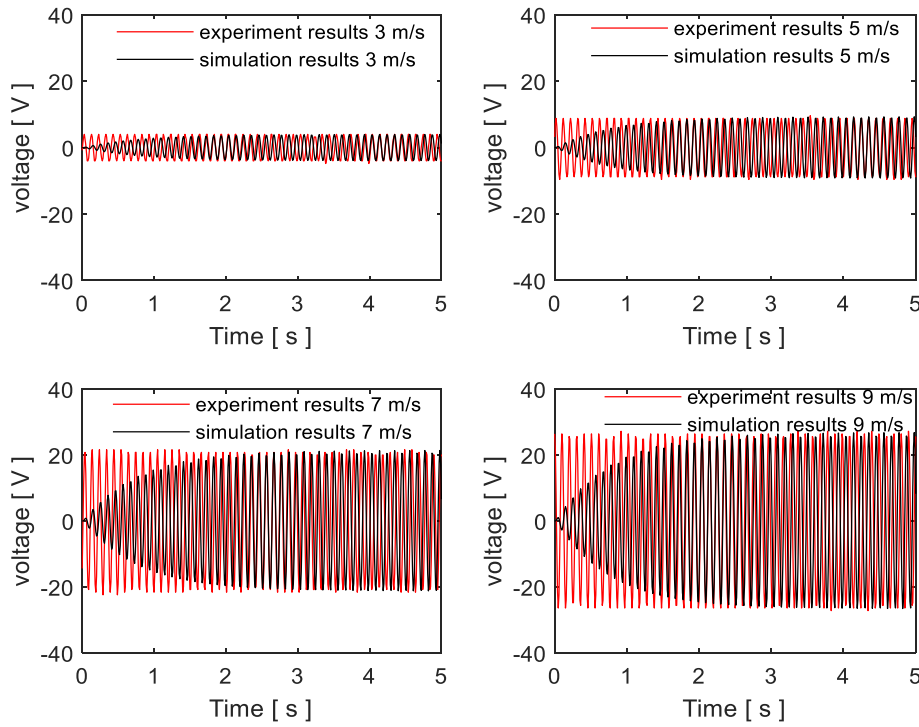


Fig. 11 Experimental and simulated voltage values as in time domain under different air velocities

#### 4.3 Comparison of simulated and experimental energy harvesting

A Simulink model is constituted using Eqs. (4). The single mode blade dynamics and piezoelectric patch dynamics are arranged as

$$\begin{aligned} \dot{q}_1 &= q_2 \\ \dot{q}_2 &= -2\xi_1\omega_{n1}q_2 - \omega_{n1}^2q_1 + \theta_1q_3 - F_x(t) \\ \dot{q}_3 &= -\frac{1}{C_pR}q_3 - \frac{\theta_1}{C_p}q_2 \end{aligned} \quad (7)$$

where  $q_1 = \eta_1$ ,  $q_2 = \dot{\eta}_1$  and  $q_3 = V(t)$ . It is assumed that the aerodynamic force input  $F_x(t)$  generated due to air

excitation affects the system at the blade resonant frequency. The constructed Matlab/Simulink model is shown in Fig. 10. The experimental and simulation results are compared in Fig. 11 for different air speeds. As seen in these figures, the voltage outputs obtained in simulations match with the experimental measured results after a converging period. Note that the aerodynamic force is separately computed for different air velocities and entered into the model for each air speed.

#### 4.4 Effect of electrical resistance

The electrical output of the piezoelectric material can be

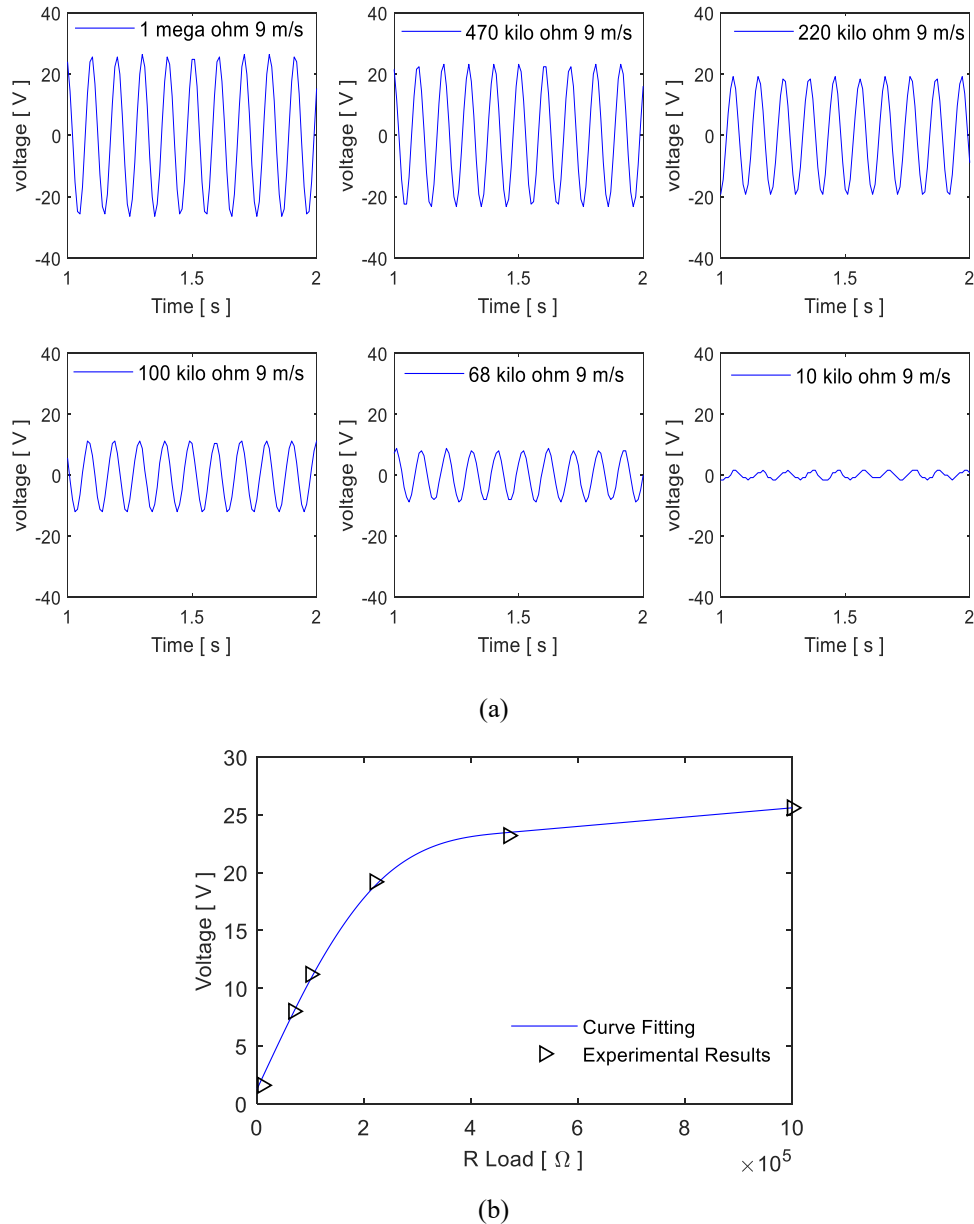


Fig. 12 Voltage output under the different electrical loads.

either voltage or current. The electrical power equation  $P = VI = V^2/R$  is used in power computations. In order to calculate the amount of energy harvested in the power form, a resistance must be connected to the piezoelectric material. At this stage, it is necessary to investigate the effect of the resistance value. Experimental results show that the voltage outputs increased at increasing electrical loads up to a certain value. Fig. 12 shows the voltage outputs under different electrical resistance loads. Moreover, Fig. 13 shows the current outputs under different electrical resistance loads. As a result, the amount of current is increased as the amount of electric load decreases to a certain value.

Table 3 lists the amounts of harvested powers computed using experimental data for different air speeds and different electrical loads. It is seen that the energy harvest is the highest in 220 kilo ohm resistance load. The variations of the power values obtained by applying the aerodynamic load at different speeds on the blade element are shown in Fig. 14. As the figure shows, the amount of energy is increased due to the increase in air velocity. It is important to decide the optimum electrical load to maximize the power output. As seen in Table 3, the resistance load of 220 kilo ohm gives the highest power output at all air speeds.

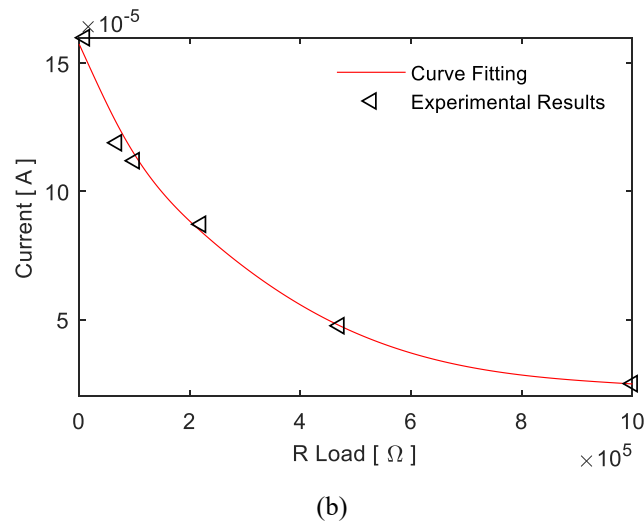
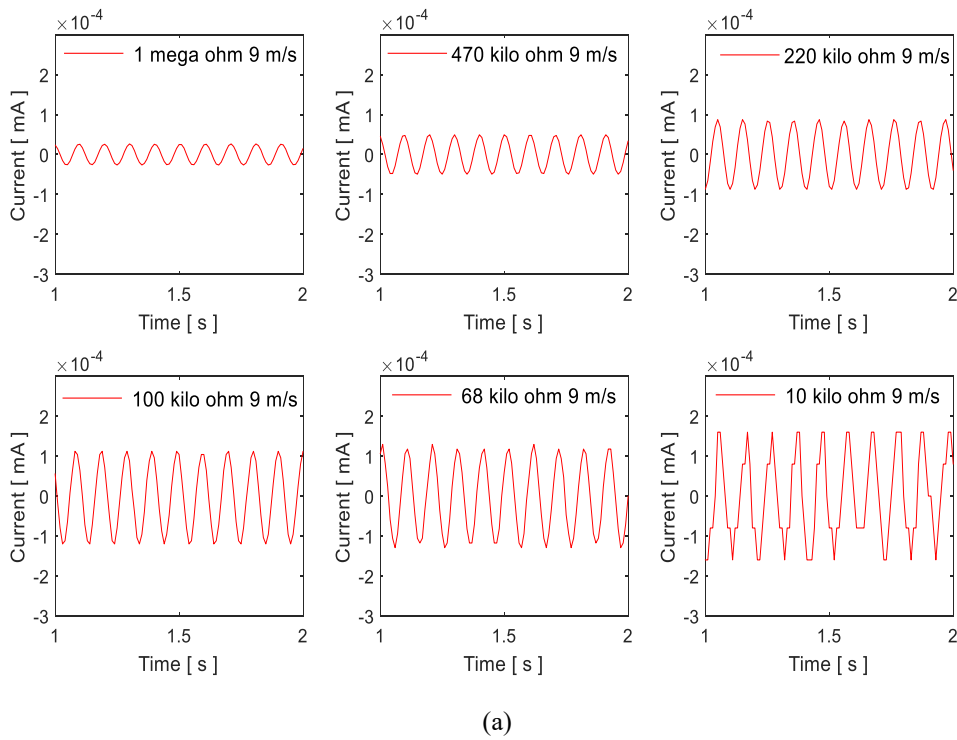


Fig. 13 Current output under the different electrical loads

Table 3 Harvested power from the blade element for investigated aerodynamic loads under different air velocities

Load (kΩ)	9 m/s (mW)	7 m/s (mW)	5 m/s (mW)	3 m/s (mW)
1000	13.10	6.91	1.54	0.32
470	21.35	13.18	3.14	0.43
220	33.51	15.56	3.18	0.58
100	25.08	15.48	2.85	0.44
68	22.70	9.22	3.01	0.32
10	6.48	5.12	1.28	0.10

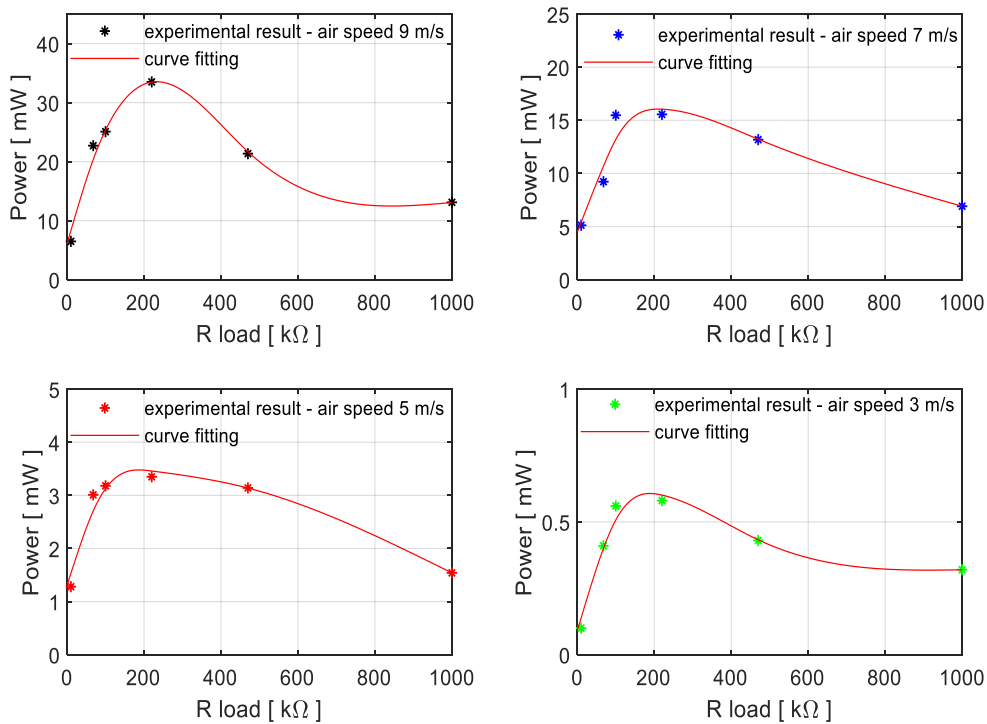


Fig. 14 Effect of different aerodynamic loads on energy harvesting.

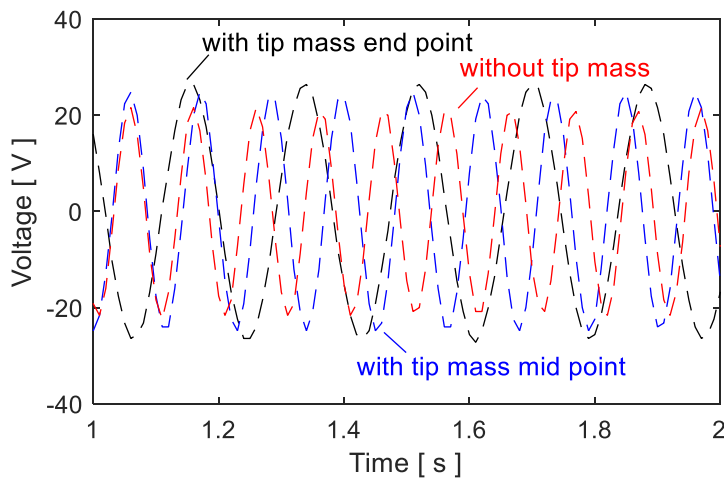


Fig. 15 Tip mass effect on the energy harvesting under the 7 m/s aerodynamic load

#### 4.5 Effect of tip mass

The variation of voltage output is observed by adding an extra mass at different locations of the blade element. Fig. 15 shows the effect of the additional mass on the energy harvesting performance of the blade element under aerodynamic load of 7 m/s. In order to examine this effect, a mass equal to 29% of the total weight of the the system is taken to the full end of the blade element. Then the same mass is added to the mid-point of the blade element and experimental measurement is taken. As shown in Fig. 15,

the amplitude value increases with the addition of mass, but the frequency reduces due to decreasing the natural frequency value. The effect on the amplitude increment of the mass added to the tip was higher than the mass added to the midpoint. However, it reduces the frequency value more than the mass added to the midpoint.

#### 5. Conclusions

This study presented an energy harvest structure for a

highly flexible blade element vibrating under the influence of aerodynamic load. To maximize the energy output of the piezoelectric patch, the blade element was forced to vibrate at its first natural frequency. The voltage, current and power outputs of the piezoelectric patch was obtained using experimental data by applying different air velocities. To characterize the proposed structure, the effects of aerodynamic load and additional mass that changes the natural frequency of the system on power output were experimentally investigated. It was shown that the resulting voltage outputs are reasonable for small electronic units. The proposed energy harvesting blade element can be safely placed in residential areas having wind potentials since it does not have any rotating parts that can create safety problems. It is also possible to design different length blade elements that have different resonant frequency and excited at different wind speeds to maximize the energy output.

## Acknowledgments

The research described in this paper no financially supported by any Foundation.

## References

- Abdelkefi, A., Yan, Z. and Hajj, M.R. (2013), "Modeling and nonlinear analysis of piezoelectric energy harvesting from transverse galloping", *Smart Mater. Struct.*, **22**(2), 025016. <https://doi.org/10.1088/0964-1726/22/2/025016>.
- Bibo, A. and Daqaq, M.F., (2013), "Energy harvesting under combined aerodynamic and base excitations", *J. Sound Vib.*, **332**(20), 5086-5102. <https://doi.org/10.1016/j.jsv.2013.04.009>.
- Bibo, A. and Daqaq, M.F., (2013), "Investigation of concurrent energy harvesting from ambient vibrations and wind using a single piezoelectric generator", *Appl. Phys. Lett.*, **102**(24), 243904. <https://doi.org/10.1063/1.4811408>.
- Bolat, F.C. and Sivrioglu, S. (2018), "Active vibration suppression of elastic blade structure: Using a novel magnetorheological layer patch", *J. Intel. Mat. Syst. Str.*, **29**(19), 3792-3803. <https://doi.org/10.1177/1045389X18799441>.
- Bolat, F.C., Basaran, S. and Sivrioglu, S. (2019), "Piezoelectric and electromagnetic hybrid energy harvesting with low-frequency vibrations of an aerodynamic profile under the air effect", *Mech. Syst. Signal Pr.*, **133**, 106246. <https://doi.org/10.1016/j.ymssp.2019.106246>.
- Bryant, M. and Garcia, E., (2011), "Modeling and testing of a novel aeroelastic flutter energy harvester", *J. Vib. Acoust.*, **133**(1), 011010. <https://doi.org/10.1115/1.4002788>.
- Bryant, M., Wolff, E. and Garcia, E. (2011), "Aeroelastic flutter energy harvester design: the sensitivity of the driving instability to system parameters", *Smart Mater. Struct.*, **20**(12), 125017. <https://doi.org/10.1088/0964-1726/20/12/125017>.
- Casciati, S., Faravelli, L. and Chen, Z. (2012), "Energy harvesting and power management of wireless sensors for structural control applications in civil engineering", *Smart Struct. Syst.*, **10**(3), 299-312. <https://doi.org/10.12989/sss.2012.10.3.299>.
- De Marqui, Jr, C. and Erturk, A. (2013), "Electroaeroelastic analysis of airfoil-based wind energy harvesting using piezoelectric transduction and electromagnetic induction", *J. Intel. Mat. Syst. Str.*, **24**(7), 846-854. <https://doi.org/10.1177/1045389X12461073>.
- Erturk, A. and Inman, D.J., (2009), "An experimentally validated bimorph cantilever model for piezoelectric energy harvesting from base excitations", *Smart Mater. Struct.*, **18**(2), 025009. <https://doi.org/10.1088/0964-1726/18/2/025009>.
- Erturk, A., Vieira, W.G.R., De Marqui, Jr, C. and Inman, D.J. (2010), "On the energy harvesting potential of piezoaeroelastic systems", *Appl. Phys. Lett.*, **96**(18), 184103. <https://doi.org/10.1063/1.3427405>.
- Javed, U., Abdelkefi, A. and Akhtar, I. (2016), "An improved stability characterization for aeroelastic energy harvesting applications". *Commun. Nonlinear Sci. Numer. Simul.*, **36**, 252-265. <https://doi.org/10.1016/j.cnsns.2015.12.001>.
- Latif, U., Abdullah, C., Uddin, E., Younis, M.Y., Sajid, M., Shah, S.R. and Mubasha, A. (2018), "Experimental and numerical investigation of the energy harvesting flexible flag in the wake of a bluff body", *Wind Struct.*, **26**(5), 279-292. <https://doi.org/10.12989/was.2018.26.5.279>.
- Sirohi, J. and Mahadik, R., (2011), "Piezoelectric wind energy harvester for low-power sensors", *J. Intel. Mat. Syst. Struct.*, **22**(18), 2215-2228. <https://doi.org/10.1177/1045389X11428366>.
- Sousa, V.C., de M Anicézio, M., De Marqui, Jr, C. and Erturk, A., (2011), "Enhanced aeroelastic energy harvesting by exploiting combined nonlinearities: theory and experiment", *Smart Mater. Struct.*, **20**(9), 094007. <https://doi.org/10.1088/0964-1726/20/9/094007>.
- Stephen, N.G. (2006), "On energy harvesting from ambient vibration", *J. Sound Vib.*, **293**(1-2), 409-425. <https://doi.org/10.1016/j.jsv.2005.10.003>.
- Tsushima, N. and Su, W. (2016), "Modeling of highly flexible multifunctional wings for energy harvesting", *J. Aircraft*, **53**(4), 1033-1044. <https://doi.org/10.2514/1.C033496>.
- Usman, M., Hanif, A., Kim, I.H. and Jung, H.J. (2018), "Experimental validation of a novel piezoelectric energy harvesting system employing wake galloping phenomenon for a broad wind spectrum", *Energy*, **153**, 882-889. <https://doi.org/10.1016/j.energy.2018.04.109>.
- Vatanserver, D., Hadimani, R.L., Shah, T. and Siores, E. (2011), "An investigation of energy harvesting from renewable sources with PVDF and PZT", *Smart Mater. Struct.*, **20**(5), p.055019. <https://doi.org/10.1088/0964-1726/20/5/055019>.
- Zhao, L. and Yang, Y. (2017), "On the modeling methods of small-scale piezoelectric wind energy harvesting", *Smart Struct. Syst.*, **19**(1), 67-90. <https://doi.org/10.12989/sss.2017.19.1.067>.

HJ